PYRITE IN THE SPRINGFIELD COAL MEMBER (V) PETERSBURG FORMATION SULLIVAN COUNTY, INDIANA

Special Report 9

State of Indiana
Department of Natural Resources
GEOLOGICAL SURVEY

SCIENTIFIC AND TECHNICAL STAFF OF THE GEOLOGICAL SURVEY

JOHN B. PATTON, State Geologist
MAURICE E. BIGGS, Assistant State Geologist
MARY BETH FOX, Mineral Statistician

COAL SECTION
CHARLES E. WIER, Geologist and Head (on leave)
RICHARD L. POWELL, Geologist and Acting Head
DONALD L. EGGERT, Geologist
HAROLD C. HUTCHISON, Geologist
MARVIN T. IVERSON, Geological Assistant

DRAFTING AND PHOTOGRAPHY SECTION
WILLIAM H. MORAN, Chief Draftsman and Head
RICHARD T. HILL, Geological Draftsman
ROBERT E. JUDAH, Geological Artist-Draftsman
ROGER L. PURCELL, Senior Geological Draftsman
GEORGE R. RINGER, Photographer

EDUCATIONAL SERVICES SECTION
R. DEE RARICK, Geologist and Head

GEOCHEMISTRY SECTION
R. K. LEININGER, Geochemist and Head
LOUIS V. MILLER, Coal Chemist
MARGARET V. GOLDE, Instrumental Analyst
CARRIE F. FOLEY, Geochemical Assistant

GEOLOGY SECTION
ROBERT H. SHAVER, Paleontologist and Head
HENRY H. GRAY, Head Stratigrapher
N. K. BLEUER, Glacial Geologist
EDWIN J. HARTKE, Environmental Geologist
JOHN R. HILL, Glacial Geologist
CARL B. REXROAD, Paleontologist

GEOPHYSICS SECTION
MAURICE E. BIGGS, Geophysicist and Head
ROBERT F. BLAKELY, Geophysicist
JOSEPH F. WHALEY, Geophysicist
CLARENCE C. HASKINS, Driller
JOHN R. HELMS, Geophysical Assistant

INDUSTRIAL MINERALS SECTION
DONALD D. CARR, Geologist and Head
CURTIS H. AULT, Geologist
MICHAEL C. MOORE, Geologist
NELSON R. SHAFFER, Geologist

PETROLEUM SECTION
LEROY E. BECKER, Geologist and Head
G. L. CARPENTER, Geologist and Associate Head
ANDREW J. HREHA, Geologist
STANLEY J. KELLER, Geologist
DAN M. SULLIVAN, Geologist
JAMES T. CAZEE, Geological Assistant
SHERRY CAZEE, Geological Assistant
WILLIAM E. HAMM, Geological Assistant

PUBLICATIONS SECTION
GERALD S. WOODARD, Editor and Head
DONNA C. SCHULTZ, Sales and Records Clerk

Pyrite in the Springfield Coal Member (V) Petersburg Formation Sullivan County, Indiana

By IKRAM U. KHAWAJA

DEPARTMENT OF NATURAL RESOURCES
GEOLOGICAL SURVEY SPECIAL REPORT 9

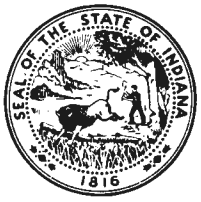

PRINTED BY AUTHORITY OF THE STATE OF INDIANA
BLOOMINGTON, INDIANA: 1975

STATE OF INDIANA
Otis R. Bowen, *Governor*
DEPARTMENT OF NATURAL RESOURCES
Joseph D. Cloud, *Director*
GEOLOGICAL SURVEY
John B. Patton, *State Geologist*

For sale by Geological Survey, Bloomington, Ind. 47401
Price $1.00

Contents

Illustrations

Tables

Pyrite in the Springfield Coal Member (V), Petersburg Formation Sullivan County, Indiana

By IKRAM U. KHAWAJA[1]

Abstract

The distribution of pyrite in the Springfield Coal Member (V), Petersburg Formation (Pennsylvanian System), was mapped underground in the Thunderbird Mine in Sullivan County, Ind. Megascopic study of data and samples from some 57 locations within the mine revealed that extreme fluctuations in the distribution of physical forms of pyrite exist. Coal in topographically high areas of a coal seam is generally thinner and contains a higher pyrite concentration. Massive lenticular pyrite occurs mainly within the upper 6 inches of the coal seam or directly below an inorganic sediment parting. Total pyrite of all forms appears to have a slightly higher concentration in the lower third of the seam. Major cleats filled with pyrite appear to be more abundant in topographically high areas. Minor cleats filled with pyrite do not seem to have any particular pattern of distribution or preference of location.

Microscopic study of four master channel samples showed that 42 percent of the pyrite is lenticular and is mainly associated with vitrinite and exinite coal macerals and with inorganic partings (mostly clay). Although clay and silt constitute more than 15 percent of the total coal seam in only a few places, as much as 47 percent of the total pyrite in the seam may be associated with them.

Pyrite crystal size and purity have a wide range and variation. Some 20 representative samples of pyrite, when studied in greater detail, showed crystal sizes ranging from 1 micron to more than 60 microns. Pyrite of museum-grade purity is rare. An electrographic analysis study of the 20 petrographic samples showed that the rate of oxidation of pyrite is inversely related to its crystallinity, crystal size, and purity. X-ray analysis of these same samples tended to substantiate these conditions.

Introduction

PURPOSE AND SCOPE

The purpose of this project was to study the distribution and associations of pyrite with other inorganic and organic materials in the coal and to relate the rate of oxidation of various forms of pyrite with inorganic and organic materials. Data resulting from this study should be useful background information that is needed to help solve air pollution problems when burning coal and acid water pollution problems resulting from water washing over pyrite-rich coal refuse.

The parameters studied and the approximate sequence of events were:

Distribution:

a. Determined relationships between the present topographic variation of the coal seam as shown in the mine tunnels and the concentration and modes of occurrence of pyrite present.
b. Determined relationships between variations in thickness of the coal seam and the concentration and modes of occurrence of pyrite.
c. Related vertical distances from the top of the coal seam and regions of high concentrations of pyrite with modes of occurrence.

Association:

a. Determined relationship between inorganic sediments and concentrations of pyrite.
b. Determined relationship between inorganic sediments and modes of occurrence of pyrite.
c. Determined relationship between kinds of maceral groups and concentration with modes of occurrence of pyrite.

Oxidation:

Determined relative rate of oxidation of iron sulfide and its relationship in terms of petrographic and X-ray analysis characteristics.

GEOLOGIC SETTING OF SAMPLE AREA

The samples used in this study were collected from the Springfield Coal Member (V) of the Petersburg Formation in the Thunderbird Mine in Sullivan County. Pyrite (iron sulfide, FeS_2) is in all coals mined in Indiana, but the Springfield Coal Member

[1]Department of geology, Youngstown State University, Youngstown, Ohio.

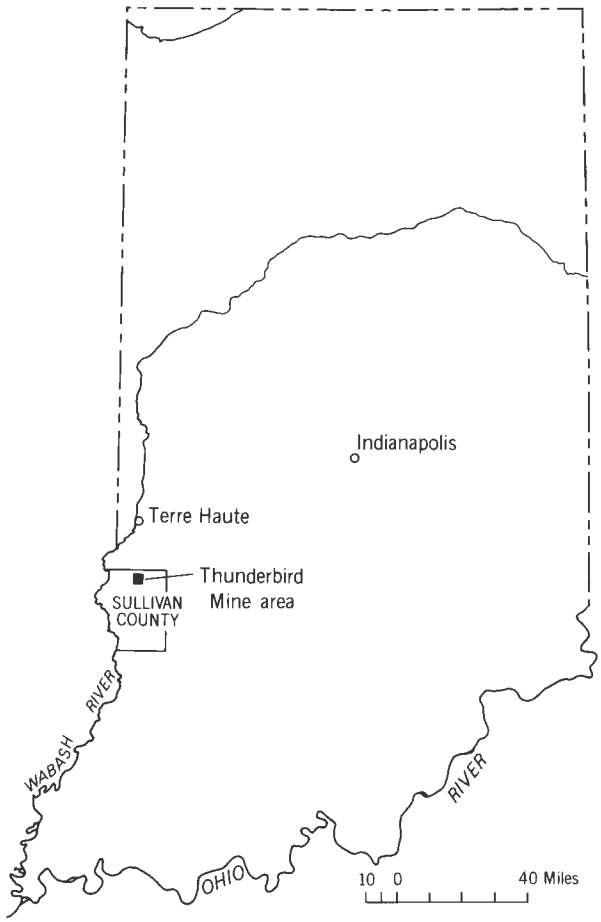

Figure 1. Map of Indiana showing location of the Thunderbird Mine area, T. 9 N., R. 9 W., Sullivan County.

(V) of the Petersburg Formation (Pennsylvanian System) was selected for this study because the pyrite content of the Springfield is among the highest in Indiana coals (Neavel, 1961, p. 67). The Thunderbird Mine area (fig. 1) was chosen because there the Springfield coal is accessible over a relatively large and continuous area.

The Thunderbird Mine began operation in 1959 in the Hymera Coal Member (VI), but the Hymera coal workings were abandoned in 1963 and at the time of this study the operation was entirely in the Springfield coal. In 1969 the Thunderbird Mine produced 1,061,890 tons of coal (Indiana Coal Association, 1970). Mining is carried out by conventional methods following the room-and-pillar plan. The main entry has been driven northward and subsequent entries branch off in both easterly and westerly directions (fig. 2). The coal is mined at a depth of about 300 feet and is brought to the surface by a conveyor belt.

The Springfield coal is the upper member of the Petersburg Formation of Pennsylvanian age. The formation averages 105 feet in thickness in the area (Waddell, 1954). Coal in the mine ranges from less than 3 feet to about 7 feet in thickness (fig. 3). The roof of the coal is generally shale, and the floor is commonly underclay. At numerous places in the mine, partings consisting mainly of inorganic sediments and pyrite are evident in the coal. The rocks in the area have a gentle westerly dip, but the Springfield coal in the mine exhibits local structural deformation (fig. 4). Shrock and Malott (1929, p. 1312) suggested that many of these structural irregularities had been formed as a result of differential compaction or subsidence of muds. This seems to be a logical explanation for the deformation in view of the absence of deformed strata both above and below the coal in the general vicinity.

PREVIOUS WORK

Because pyrite in coal affects marketability, attention was directed early toward its presence, distribution, and nature. Ashley (1919) discussed different modes of occurrence of pyrite, and Thiessen (1919) studied the occurrence of finely disseminated pyrite in coal. Tucker (1919) gave an account of pyrite in Ohio coal. Yancey and Fraser (1921) presented an excellent descriptive account of physical forms of pyrite in coal. Numerous other papers on the distribution and description of the different forms of pyrite have been published; notable among these are the papers by Newhouse (1927), Yancey and Parr (1927), Cady (1935), Sprunk and O'Donnell (1942), and Gray and others (1963). This widespread work has produced considerable information with respect to the sulfur content of coal, but the relationships between the pyritic materials and other materials, such as organic matter and clay minerals or other inorganic materials associated with them, have not been investigated thoroughly.

Dove (1919) discussed various modes of occurrence of pyrite for Indiana coals. Holbrook (1919) studied the removal of pyrite from Indiana coals and discussed briefly its mode of origin. The relationship of petrography and sulfur content of Indiana coal was briefly investigated by Neavel (1961), who directed his study toward coal petrography and did not attempt to describe the forms of sulfur in any detail.

Because pyrite in coal oxidizes to sulfate and produces sulfuric acid in stream waters near the mines, the rate and amount of oxidation have been of some concern. Stokes (1907) conducted experiments on the oxidation of pyrite. Winchell (1907) and Gottschalk and Buehler (1912) also described experiments of pyrite oxidation. Powell and Parr (1919, p. 8) concluded that bacteria and time are the major rate-controlling factors in iron sulfide oxidation.

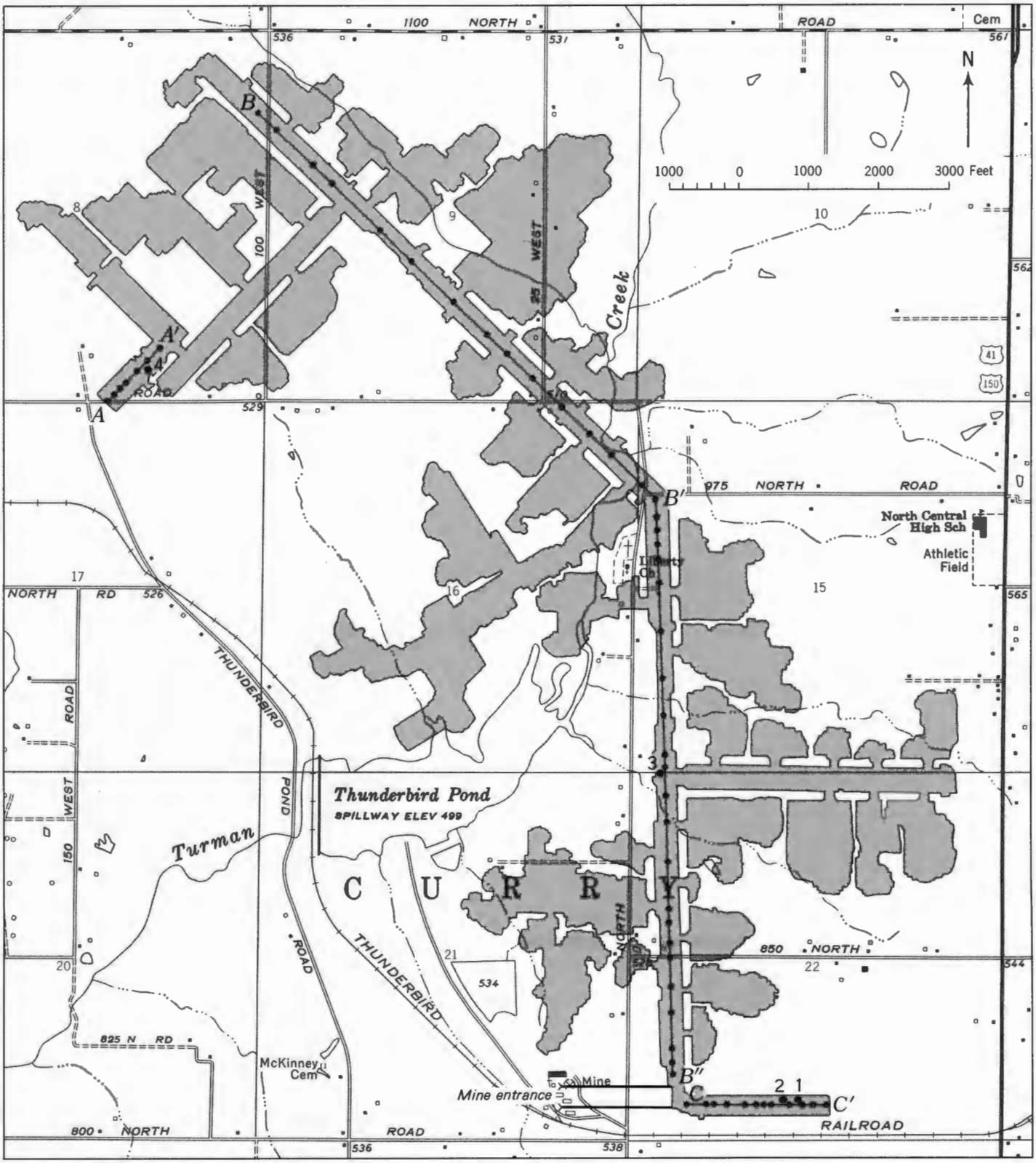

Figure 2. Map showing Thunderbird Mine workings and locations of the four master columns and 57 sites that were studied.

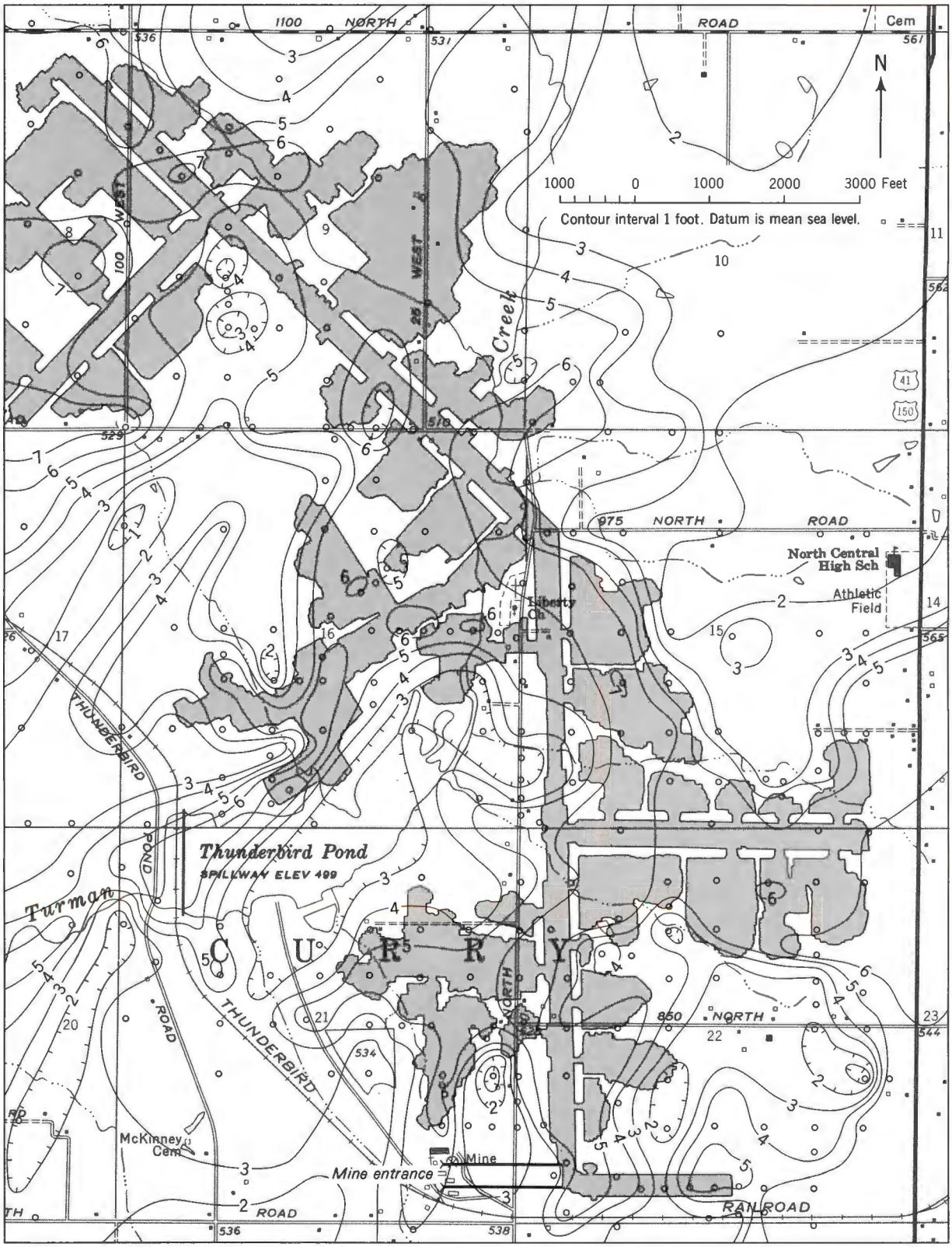

Figure 3. Map of the Thunderbird Mine area showing thickness of the Springfield Coal Member (V). Location of coal drill holes is shown with open circles.

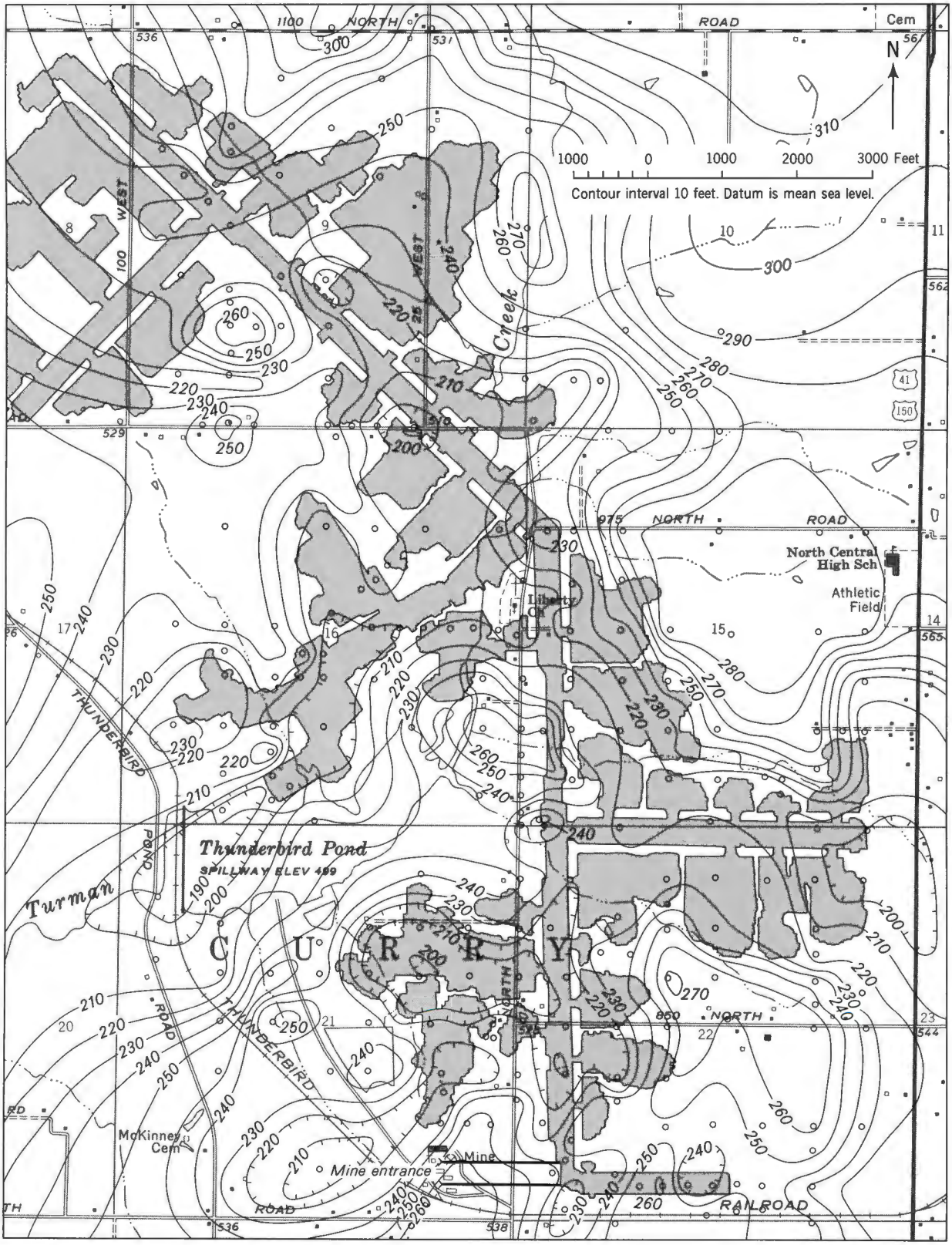

Figure 4. Map of the Thunderbird Mine area showing structure contours on top of the Springfield Coal Member (V). Location of coal drill holes is shown with open circles.

In subsequent years the problem of acid drainage has received more attention, and consequently knowledge concerning iron sulfide oxidation has substantially increased. Nelson and others (1933) were able to establish a direct relationship between size of particles and rate of oxidation of iron sulfide. Bain (1935) suggested that sodium and potassium salts accelerate oxidation. Stenhouse and Armstrong (1952) studied aqueous oxidation of pyrite; their conclusions were later largely confirmed by McKay and Halpern (1958). Their work and that of Braley (1960) and Sato (1960) produced information on the kinetics of sulfide-to-sulfate oxidation. Rossetti and Cesini (1957) pointed out that mineralogy, a somewhat neglected aspect of previous experimental work, also plays an important part in the kinetics of sulfide-to-sulfate reactions.

About 50 years ago Powell and Parr (1919) suggested that sulfide oxidation in coal appears to be accelerated by bacteria. Studies on the role of microorganisms in the oxidation of iron sulfide have been done at various places. Those of greatest importance have been made at the West Virginia Engineering Experiment Station (1930-53), the Mellon Institute (1946-present), and Brigham Young University (1958-present). Silverman, Rogoff, and Wender (1963) and Silverman and Ehrlich (1964) demonstrated that particle size and rate of oxidation of iron sulfide are inversely proportional. They also concluded (1963, p. 123) that bacteria, especially *Ferrobacillus ferroxidans,* greatly accelerate the rate of sulfide oxidation. Silverman and Ehrlich (1964) suggested that the crystal structure of iron sulfide is an important factor in governing its susceptibility to oxidation in the presence of bacteria. They also suggested (1964, p. 182) that gangue (associated minerals) may have a marked influence on the rate of oxidation of iron sulfide. Although bacteria do accelerate the oxidation of iron sulfide, oxidation can start in their absence (Silverman and Ehrlich, 1964, p. 181).

ACKNOWLEDGMENTS

This study began as a doctoral thesis at Indiana University. Acknowledgment is due Dr. Charles E. Wier, who suggested this study, helped while it was in progress, and made arrangements with the Ayrshire Coal Corp. [Amax Coal Co.] for collecting samples and relevant data. Thanks are also due Mr. Reuben Tucker, superintendent of the Thunderbird Mine. The late Dr. Carl W. Beck advised in the X-ray study; Mr. Marvin T. Iverson helped with the fieldwork; and Mr. Harold C. Hutchison and Miss Susan Hertz helped greatly in preparing this report from the doctoral thesis. The thesis work was partly sponsored by the Indiana Geological Survey.

Distribution and Association of Pyrite in the Springfield Coal Member (V)

In this report both megascopic and microscopic studies of selected samples are used to determine the distribution of pyrite in the coal and the association of the pyrite with other inorganic materials and maceral groups.

MEGASCOPIC CLASSIFICATION OF PYRITE

To map and study megascopically the distribution and association of pyrite in the mine, it was necessary to use a limited number of descriptive categories. The system of classification of the pyrite that was used (table 1) was not new but was modified from the work of others.

DISTRIBUTION OF PYRITE AS DETERMINED BY MEGASCOPIC METHODS

The Main North, Main East, and 11b West entries (fig. 2) of the Thunderbird Mine had large areas of

Table 1. Classification of pyrite for megascopic study

Mode of occurrence	Description
Lenticular	Occurs as lenslike shapes parallel to bedding of the coal. Pyrite exhibits both euhedral and anhedral types.
Massive	Mostly pure pyrite.
Mixed	About 50 percent pyrite, mixed with other inorganic sediments and coal macerals.
Disseminated	Small percentage of pyrite disseminated through inorganic sediments.
Cleat filling	Occurs in thin vertical sheets oriented more or less normal to the bedding of the coal. Usually pure pyrite and generally euhedral.
Major	Cleats 6 inches or more in length.
Minor	Cleats less than 6 inches in length.

OVERSIZED DOCUMENT

Now located at end of publication.

Table 2. Classification of pyrite for microscopic study

Type	Description
Lens	Lens-shaped parallel to the bedding of the coal seam. May be nearly pure massive pyrite or pyrite mixed with inorganic and organic sediments.
Dendrite	Appears to have formed by branching growth, oriented normal or at an angle to the bedding of the coal.
Veinlet	Thin veins; generally pure pyrite. Oriented more or less normal to the bedding of the coal.
Euhedral crystal	Crystal faces are distinct; occurs as isolated crystals, commonly found in association with fusinite, or as aggregates where crystals have coalesced to some extent.
Bleb	Pyrite of limited extent, not fitting into any of the other types; includes small spherical shapes and small irregular masses.

exposed coal and were selected for mapping the distribution of pyrite. Four traverses were made in the mine; these are identified as AA′, BB′, B′BB″, and CC′ (pl. 1). On plate 1 each of the 57 locations is identified as belonging to a particular traverse. Individual locations were selected to provide representative sampling and study in relation to the topography and thickness of the coal seam.

At each sample location a column 1½ to 2 feet wide was cleaned as a fresh face of the seam. The column was measured from top to bottom and plotted on a reduced scale (1 inch equals 1 foot). The coal columns (pl. 1) were plotted with vertical displacement relative to their local position as high, low, or intermediate. The pyrite occurrence was recorded with reference to location, topographic position relative to structure on the coal, thickness of coal, type of roof and bottom material, and inorganic sediment partings. This procedure permitted the study of possible relationships between topographic variation, thickness of coal, and vertical distance from the roof to concentrations and physical forms of pyrite present.

Data collected from the 57 locations reveal that there are extreme variations in the distribution and mode of occurrence of pyrite from site to site and that a quantitative comparison is difficult. But relationships do exist between topographic and thickness variations of the coal seam and the distribution and concentrations of various physical forms of pyrite (pl. 1). Coal in topographically high areas is generally thinner than coal in associated low and level areas, and, conversely, thicker coals are in the low areas. Massive lenticular pyrite is more common in topographically high areas than in the associated low or nearly level areas. These high areas also have a high concentration of concretionary bodies in the roof material. The concretionary bodies extend down into the upper part of the coal in places and consist primarily of clay, pyrite, and siderite. Mixed and disseminated pyrite of small crystal size does not significantly vary in its distribution with respect to topographic variation. The percentage of total pyrite is slightly greater in thinner coal and in topographically high areas.

Data on vertical distribution, concentration, and mode of occurrence of pyrite versus distance from the top of the coal seam also allow some conclusions. Massive lenticular pyrite occurs mainly either within the top 6 inches of the seam or directly below an inorganic sediment parting. Pyrite of finer crystal size is distributed rather evenly with a slight preference for the lower third of the coal seam. Total pyrite of all forms appears to have a slightly higher concentration in the lower third of the coal seam. Minor cleats filled with pyrite do not seem to have any particular pattern of distribution or preference of location, but major cleats filled with pyrite appear to be more abundant in a topographically high area. Cleats filled with calcite have no particular distribution pattern and are present in most locations throughout the coal seam.

MICROSCOPIC CLASSIFICATION OF PYRITE

Microscopic study of the distribution and association of pyrite necessitates a different system of classification from that used megascopically. The classification shown in table 2 was used in the laboratory studies conducted on the selected samples.

DISTRIBUTION AND ASSOCIATION OF PYRITE AS DETERMINED BY MICROSCOPIC METHODS

To study the microscopic association and distribution of pyrite, four master columns were channeled: columns 1 and 2 from the Main East entry, column 3 from the Main North entry, and column 4 from the

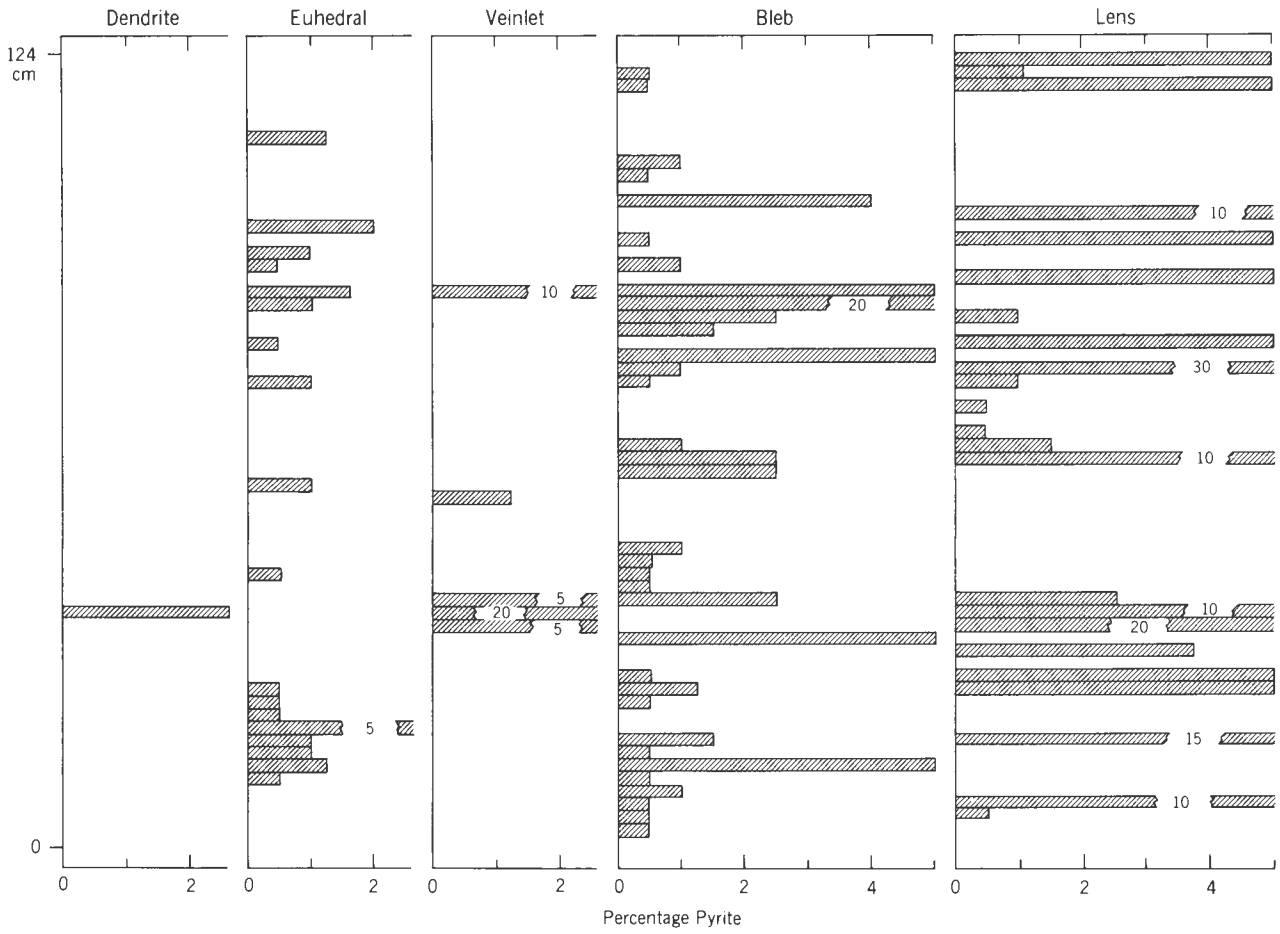

Figure 5. Vertical distribution of pyrite types in master column 1.

11b West entry (fig. 2). These master columns were investigated through a binocular microscope by using a 60 X magnification. In addition, portions of each column were further studied with an ore microscope by using 100 X and 250 X magnifications. The blocks selected for study under the ore microscope were mounted and polished normal to the bedding planes of the coal seam. Quantitative estimation was done by a point-count technique using 2-centimeter increments. The 2-centimeter increment was used because it was small enough to show meaningful vertical variation in the petrographic composition of the coal and because the combined increments could be plotted easily on a page for graphic representation.

A graphic representation of the distribution of pyrite types in the coal seam were plotted (figs. 5, 6, 7, and 8). The vertical coordinate represents the thickness of the coal, and the horizontal coordinate in each column represents the percentage of pyrite. Each figure is divided into five columns, each column representing a particular pyrite type based on the classification given in table 2.

Total pyrite (all microscopic types combined) in relation to benches of dominant coal maceral groups was plotted for the same master columns (figs. 9, 10, 11, and 12). These benches were selected if a certain maceral group exceeded 50 percent, or if the amount of a certain maceral group (other than vitrinite) was abnormally high for a particular location, whether or not it exceeded 50 percent. For example, certain benches were labeled fusinite if they had more than 20 percent fusinite in a location at which the amount of fusinite did not exceed 3 or 4 percent in other benches.

Data presented in figures 5, 6, 7, and 8 and in tables 3 and 4 allow one to arrive at certain conclusions. The lenticular type dominates all others in total percentage of pyrite; about 42 percent of the pyrite in the four master columns is in lenses. Individual bands as much as 6 centimeters thick are present (figs. 6 and 10). Blebs are uniformly distributed and constitute the second highest concentration of pyrite. High concentration of lenticular pyrite generally coincides with correspondingly high concentra-

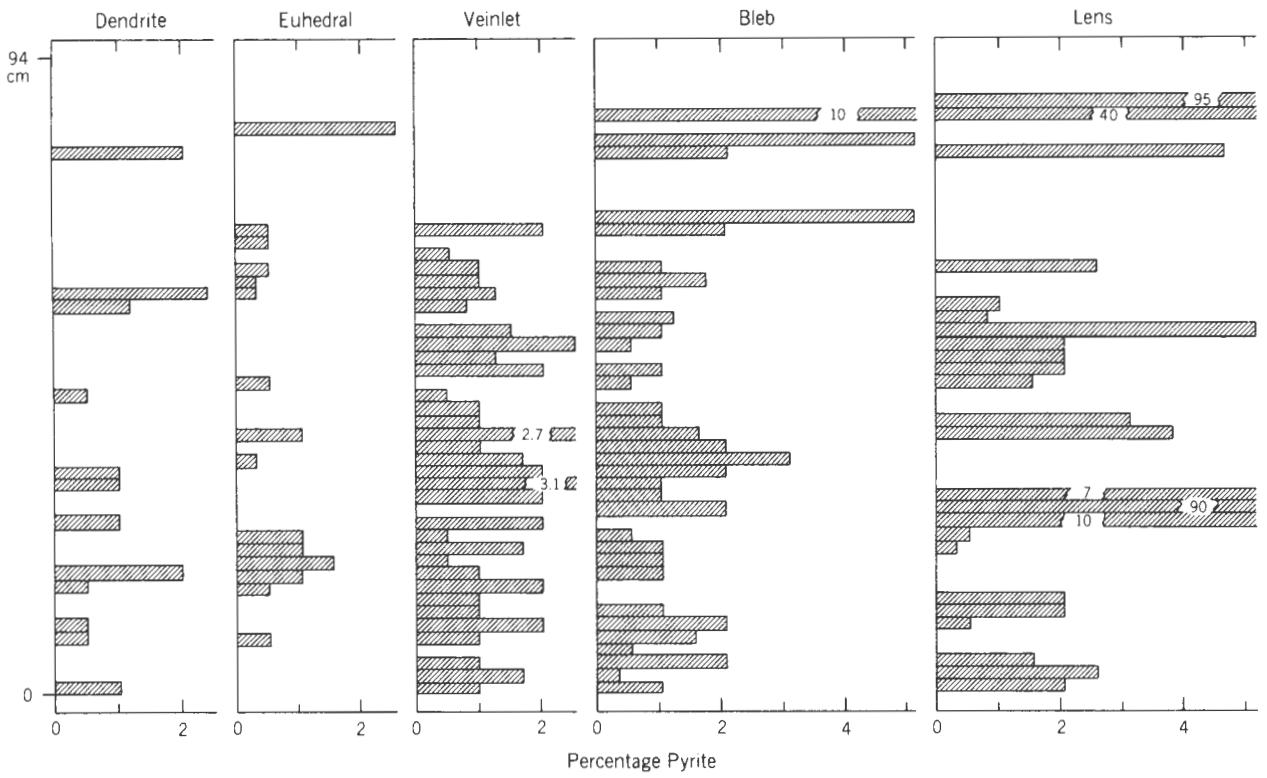

Figure 6. Vertical distribution of pyrite types in master column 2.

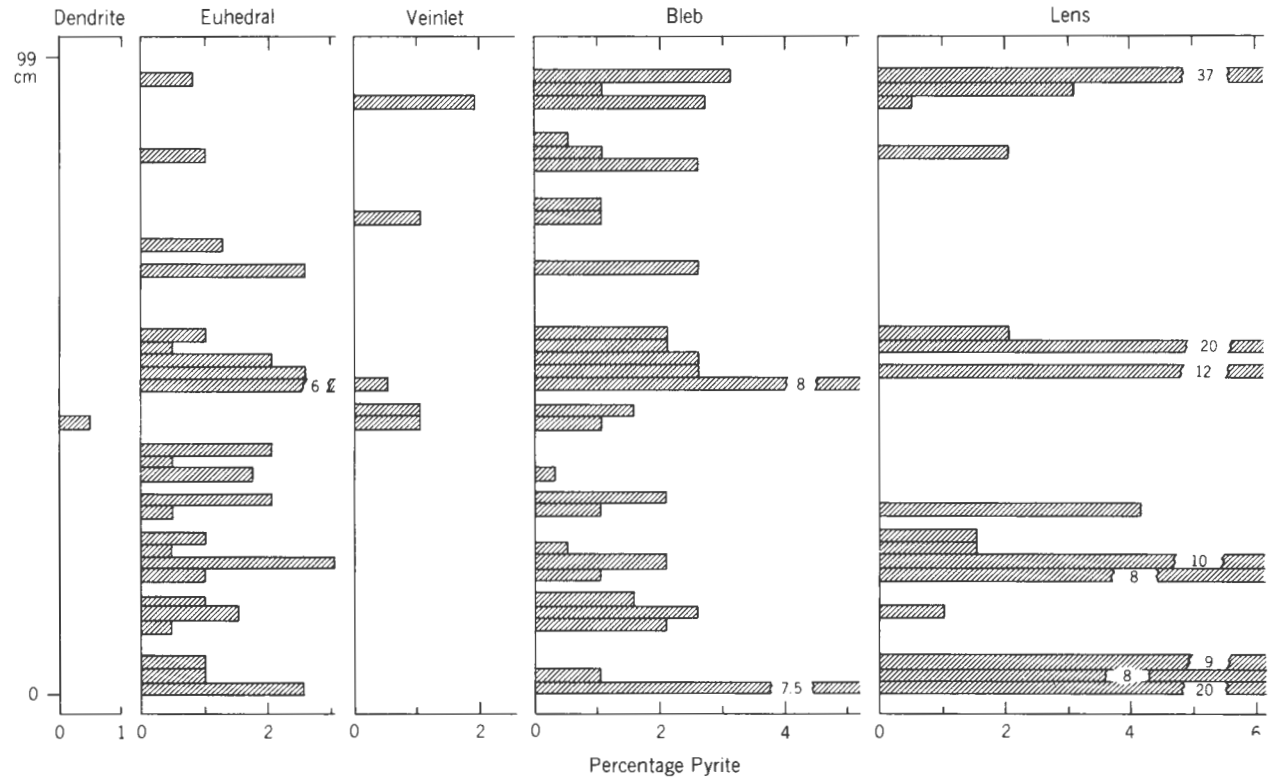

Figure 7. Vertical distribution of pyrite types in master column 3.

Figure 8. Vertical distribution of pyrite types in master column 4.

tion of blebs. Pyrite veinlets are more localized, and their high concentration generally corresponds to a zone of high concentration of the lenticular pyrite. The euhedral type is a minor constituent and appears to be concentrated in the lower and upper parts of the seam in columns 1 and 2, but it is more abundant and uniformly distributed in columns 3 and 4. The dendritic type is a minor part of the samples. Where there is a high concentration of other pyrite types, dendrites are more common (fig. 6).

Table 3. Association of pyrite types with coal maceral groups

Type	Master column 1			Master column 2			Master column 3			Master column 4		
	Pyrite			Pyrite			Pyrite			Pyrite		
	Percent of total coal	Percent of total pyrite	Percent of pyrite type	Percent of total coal	Percent of total pyrite	Percent of pyrite type	Percent of total coal	Percent of total pyrite	Percent of pyrite type	Percent of total coal	Percent of total pyrite	Percent of pyrite type
Bleb:												
Vitrinite - - -	0.33	7.2	31	0.45	5.3	41	0.66	12.7	58	0.4	10.9	40.5
Fusinite - - -	0.32	7	30	0.28	3.3	25	0.23	4.4	21	0.15	4.2	15.7
Exinite - - - -	0.42	9	39	0.38	4.3	34	0.24	4.5	21	0.44	11.8	43.8
Total bleb - - - -	1.07	23.2	100	1.11	12.9	100	1.13	21.6	100	0.99	26.9	100
Veinlet:												
Vitrinite - - -	0.33	7.2	51	0.62	7.3	68	0.08	1.5	72	0.16	4.4	61
Fusinite - - -	0	0	0	0	0	0	0	0	0	0	0	0
Exinite - - - -	0.32	7.1	49	0.28	3.3	32	0.03	0.59	28	0.1	2.8	39
Total veinlet - - -	0.65	14.3	100	0.90	10.6	100	0.11	2.09	100	0.26	7.2	100
Lens:												
Vitrinite - - -	0.90	20.5	48	0.69	8.1	36	1.9	36.1	76	0.79	20.9	43.2
Fusinite - - -	0.16	3.5	8	0.02	0.2	1	0.16	3.1	7	0.07	1.7	3.6
Exinite - - - -	0.88	19.1	44	1.2	14	63	0.42	8	17	0.97	25.8	53.2
Total lens - - - -	1.94	43.1	100	1.91	22.3	100	2.48	47.2	100	1.83	48.4	100
Euhedral:												
Vitrinite - - -	0.08	1.8	25	0.06	0.69	19	0.33	6.3	45	0.23	6.1	35.7
Fusinite - - -	0.18	4	55	0.15	1.8	49	0.27	5.2	38	0.33	8.7	51
Exinite - - - -	0.06	1.4	20	0.1	1.2	32	0.12	2.4	17	0.09	2.3	13.3
Total euhedral - -	0.32	7.2	100	0.31	3.69	100	0.72	13.9	100	0.65	17.1	100
Dendrite:												
Vitrinite - - -	0.02	0.5	43	0.16	2	62	0.01	0.2	100	0.01	0.27	66.7
Fusinite - - -	0	0	0	0	0	0	0	0	0	0	0	0
Exinite - - - -	0.03	0.9	57	0.09	1.1	38	0	0	0	0.005	0.13	33.3
Total dendrite - -	0.05	1.4	100	0.25	3.1	100	0.01	0.2	100	0.015	0.40	100
Pyrite associated with inorganics		10.8	—		47.4	—		15.0	—		—	—

Table 4. Association of total pyrite with coal maceral groups

Associated maceral group	Master column 1		Master column 2		Master column 3		Master column 4		Average of columns	
	Percent of total pyrite	Percent of maceral in coal	Percent of total pyrite	Percent of maceral in coal	Percent of total pyrite	Percent of maceral in coal	Percent of total pyrite	Percent of maceral in coal	Percent of total pyrite	Percent of maceral in coal
Vitrinite - - -	37.2	24.6	23.4	70.6	56.8	80.6	42.6	44.4	40.0	55.0
Fusinite - - -	14.5	18.5	5.3	6	12.7	12.3	14.6	17.2	11.8	13.5
Exinite - - - -	37.5	52.3	23.9	17	15.5	6.1	42.8	38.4	29.9	28.5
Inorganic- - -	10.8	4.6	47.4	6.4	15	1	0	0	8.3	3.0

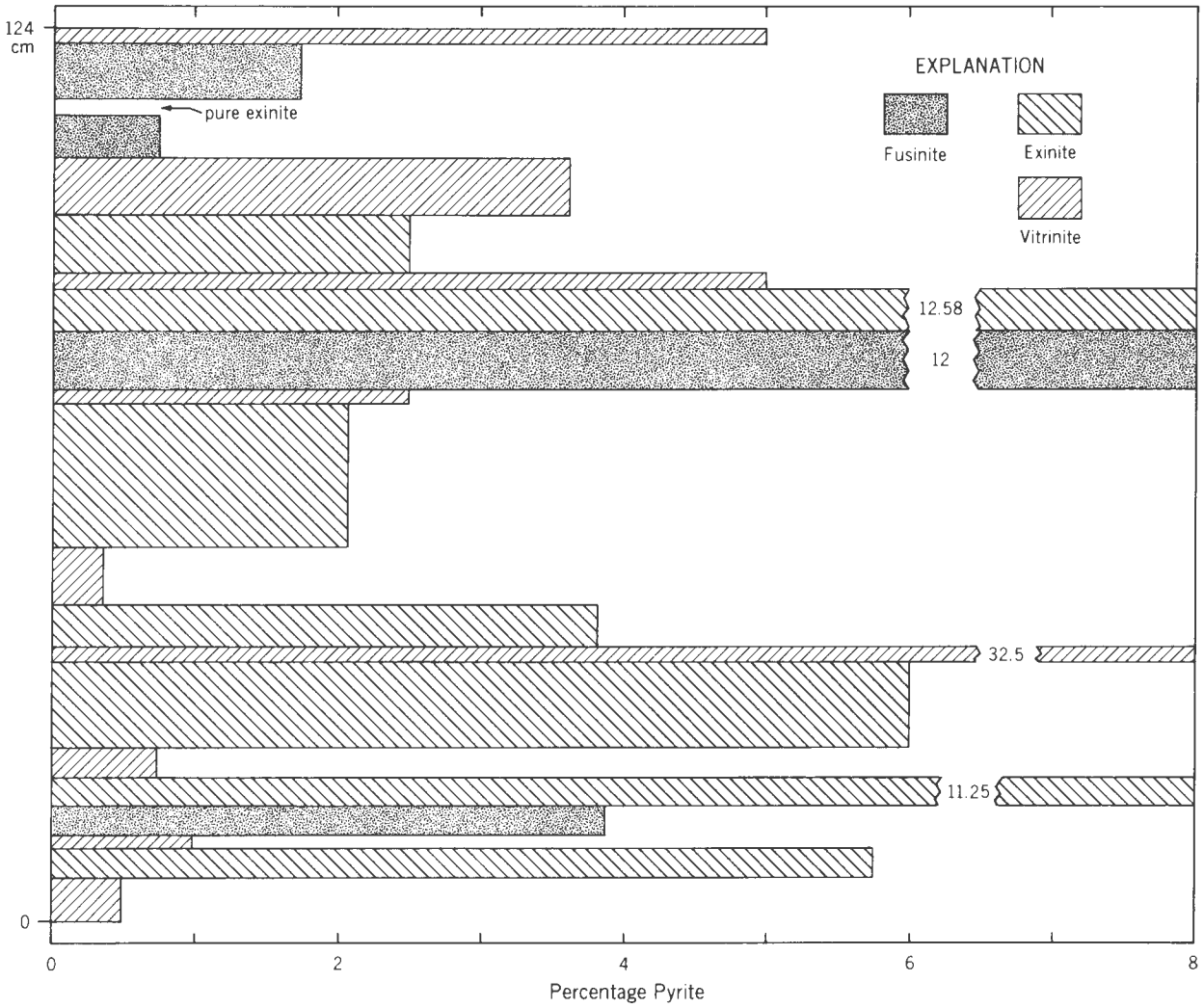

Figure 9. Association of pyrite with coal macerals in master column 1.

Inorganic sediments have a much higher concentration of pyrite in association with them than any of the coal maceral groups have. Although the inorganic sediments constitute more than 15 percent of the entire coal seam in only a few places, they may have as much as 47 percent of the total pyrite associated with them (table 4). The most common type of pyrite associated with inorganic sediments is the lens. The euhedral type is also present with inorganic sediments in significant amounts, but the amount of blebs, veinlets, and dendrites is insignificant.

When one considers the relation of pyrite to coal maceral groups (figs. 9-12 and tables 3 and 4), the major portion of the pyrite appears to be associated with vitrinite and exinite. This relationship changes significantly, however, when the association is considered from a different viewpoint. If percentages of vitrinite, exinite, fusinite, and inorganic sediments in the coal are calculated, the inorganic sediments, followed by exinite and fusinite, have the highest concentration of pyrite (table 4). Blebs are equally distributed in vitrinite and exinite zones, but their concentration in the fusinite zones is less (table 3). The euhedral type is primarily associated with fusinite zones, and the vitrinite zones have a higher share of euhedral type than the exinite zones do. Cleat fillings and dendritic modes of occurrence are predominantly associated with vitrinite zones and are almost nonexistent in the fusinite zones (table 3). Lenses of pyrite are primarily associated with vitrinite and exinite zones and rarely with fusinite zones (table 3).

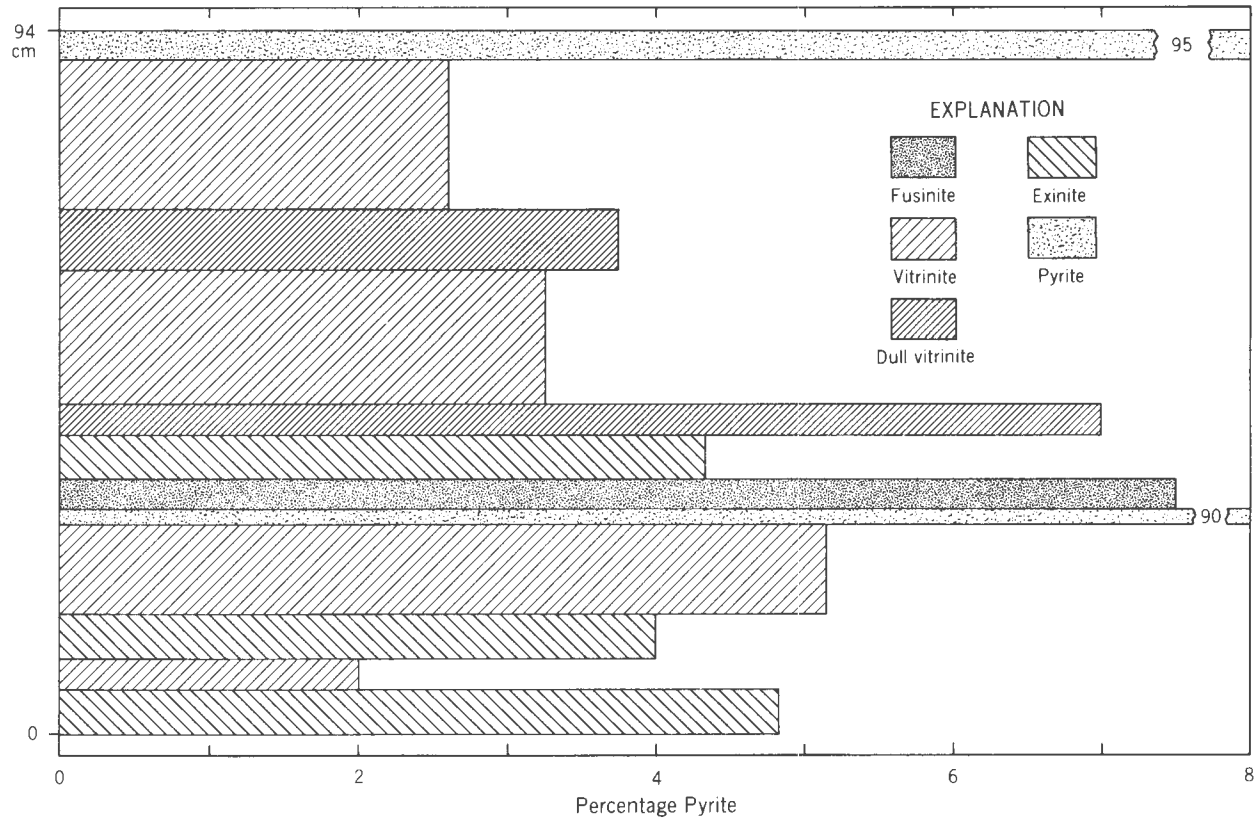

Figure 10. Association of pyrite with coal macerals in master column 2.

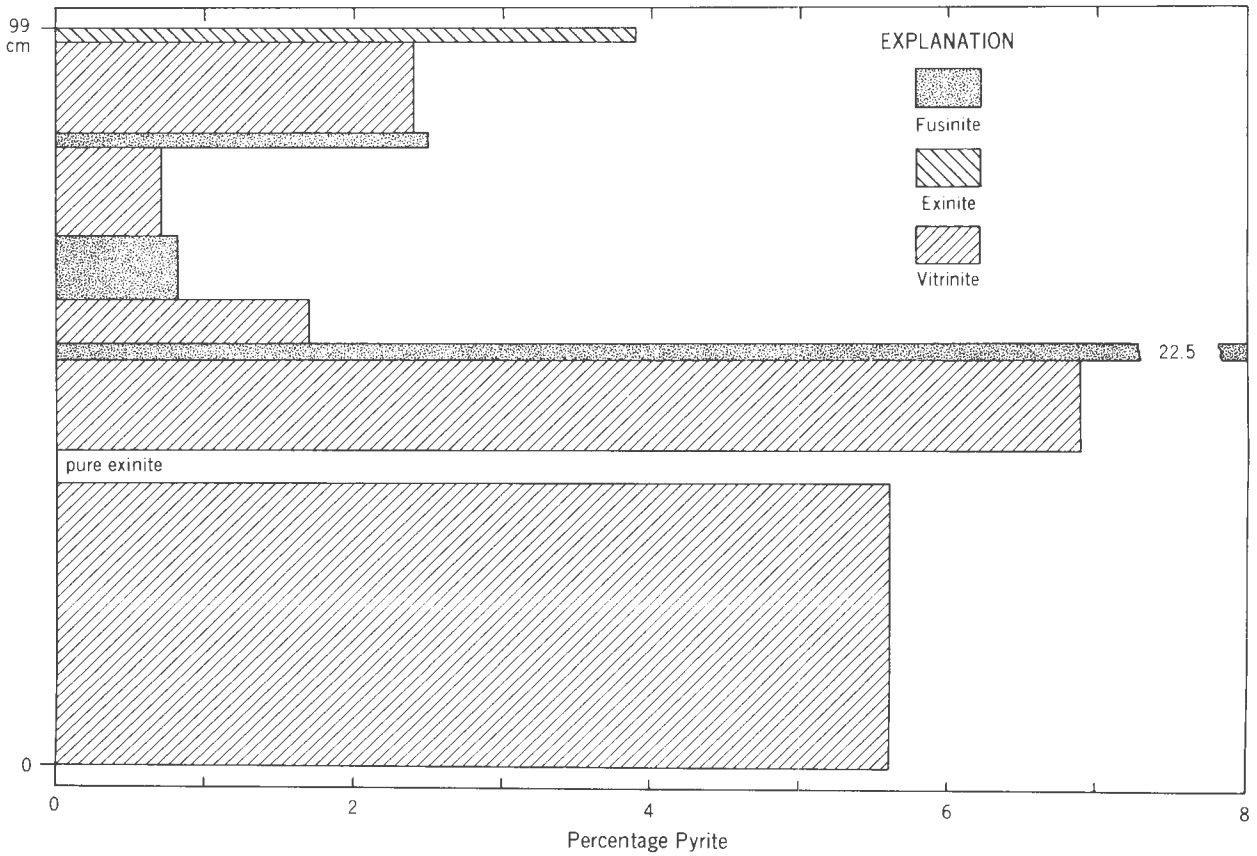

Figure 11. Association of pyrite with coal macerals in master column 3.

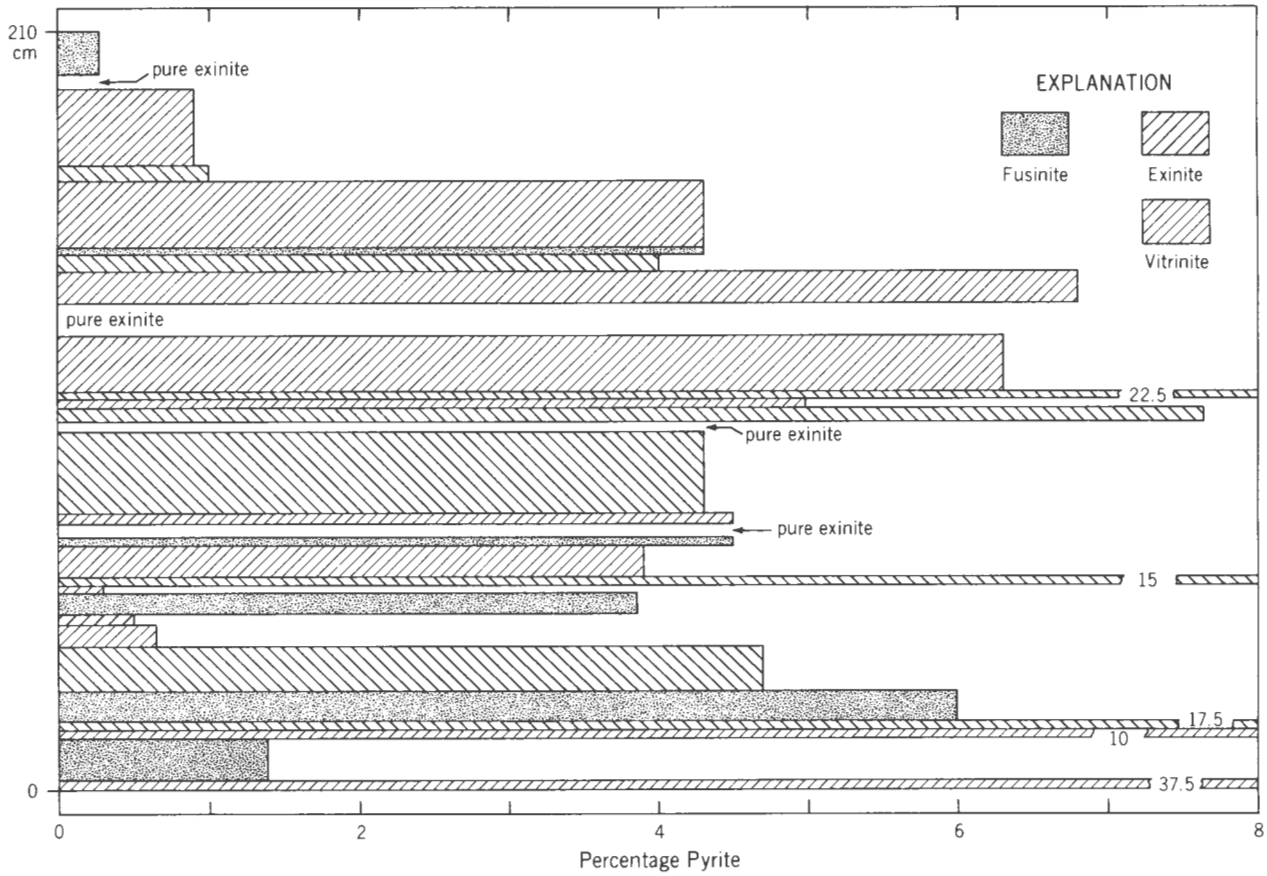

Figure 12. Association of pyrite with coal macerals in master column 4.

Oxidation of Pyrite

To relate mode of occurrence and types of pyrite with rate of oxidation, representative pieces of pyrite were characterized by means of standard petrographic techniques and oxidized in an electrograph. X-ray analyses of samples that oxidized at different rates were made. Additional samples were collected from the Springfield Coal Member (V) in strip mines in Sullivan, Greene, Pike, and Gibson Counties. Eighty-seven grab samples of pyrite-rich coal, including those from the Thunderbird Mine, were given a cursory examination. Representative pieces of these samples were analyzed by an X-ray diffractometer for identification of pyrite and associated minerals. Minerals that could be identified with certainty included pyrite, calcite, and siderite. In many samples a peak was noted for "d" spacing of about 10Å. This peak was interpreted as denoting a degraded clay mineral, possibly degraded illite. Marcasite was not detected on the X-ray charts.

PETROGRAPHIC IDENTIFICATION AND SELECTION

Twenty representative and typical samples of pyrite then were selected and isolated from the 87 coal samples. These 20 samples were prepared into blocks (with dimensions ranging from ½ to 1½ inches) and embedded in bioplastic for polishing and handling in preparation for petrographic study and later for electrographic and X-ray analyses. The objective of this petrographic study was to examine in further microscopic detail the type of pyrite, its approximate crystal size, and its apparent purity. A Leitz ortholux microscope was used for this polished surface study. Magnifications of 375 X and 900 X were used.

Samples studied have been identified in the field as cleat filling, as massive lenticular, or as disseminated pyrite (table 1). Pyrite in cleats is generally crystalline and shows crystal elongation perpendicular to the cleat wall. In places the crystals overlap each other in a steplike manner that signifies successive formation of the crystals. Calcite is also a common mineral in cleats. In some places pyrite fillings in cleats are encrusted by calcite.

Massive pyrite and disseminated lenticular pyrite contain small lens-shaped bodies of crystalline pyrite parallel to the bedding plane and smaller disseminated bodies mixed with considerable organic and some inorganic materials (clay or silica) in varying proportions. Tucker (1919) observed that pyrite in cleats may cut across a lenticular band of pyrite but that

the reverse does not occur. Tucker's observation was found to be true in this study. In a few samples part of the pyrite in lenticular bands appeared to have undergone recrystallization. Pyrite in finely disseminated form commonly occurs as small globules or clusters of globules (either euhedral or anhedral), which commonly range in diameter from 20 to 50 microns, but a few are as small as 1 micron. The greatest concentrations of disseminated globules occur in vitrinite.

Euhedral crystals of pyrite are commonly associated with fusinite bands. Complete replacement of plant material by pyrite is evident at numerous places in many samples, and pyrite commonly fills the organic cell structure in fusinite. Pyrite crystal size and purity have a wide range and variation. Euhedral pyrite ranges from more than 60 microns to less than 1 micron in size. The largest crystal size is most commonly associated with the cleat fillings, and the lenticular lenses generally have pyrite of a much smaller crystal size. Recrystallized pyrite in lenticular lenses has a larger crystal size than that immediately surrounding it.

Pyrite of museum-grade purity is rare. Pyrite in cleat fillings is much more pure than that in lenticular lenses. In fact, pyrite bordering a lenticular lens is most impure. This impure pyrite generally occurs in a band about 100 microns wide on both sides of the lens. Recrystallized pyrite in lenticular lenses has a much higher purity than that which surrounds it. A brief petrographic description of each of the 20 samples studied is given in the appendix. Many blocks contained varied pyrite types and these were noted. On the basis of the petrographic study, pyrite of varying degrees of purity and crystal size were used for the electrographic and X-ray studies.

ELECTROGRAPHIC ANALYSIS

To compare petrographic properties with rate of oxidation, it was necessary to find a method for measuring rate of oxidation of pyrite that would not result in a breaking up or a complete loss of the sample so that the sample could be used for petrographic and X-ray studies. A survey of the literature revealed that the rate of oxidation of pyrite could be studied by using a modified electrographic method of testing. Fritz (1929) and Glazunov (1929) independently published methods using electrolytic solution of a metal specimen to drive its ions into a paper reaction medium. They developed the method primarily for metallurgic studies. Since oxidation of pyrite starts at the exposed surfaces, the method involves a surface printing based on electrolytic solution of the surface and acceleration of dissolved ions to provide transfer into a printing medium. Such a transfer is rapid, under instant control, and uses neutral noninterfering electrolytes for dissolving the surface and an electric field which acts to prevent lateral diffusion of ionic material. Pyrite is a conducting material, and its oxidation product, $FeSO_4 \cdot nH_2O$, is ionizable. In $K_4Fe(CN)_6$ a suitable electrolyte and fixing which would not dissolve pyrite but would dissolve $FeSO_4 \cdot nH_2O$ and react with the iron to give a blue color was found.

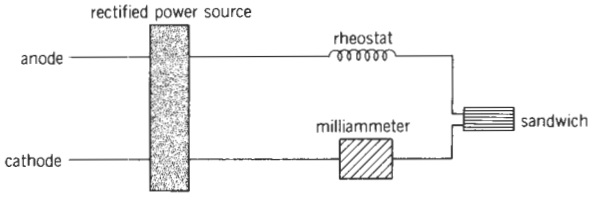

Figure 13. Circuit arrangement used in electrographic analysis.

Hermance and Wadlow (1951) described the electrographic method in great detail. Basically, the electrograph consists of two metal (or conducting) surfaces between which is andwiched a layer of absorbent printing film or paper moistened with electrolyte and fixing reagent. When the metal surfaces are connected to a potential source, they form the anode and the cathode of an electrolytic cell, and ions from the specimen, which is the anode, move into the printing medium (paper) and react with the fixing reagent to produce a colored print. Factors which must be standarized are current, voltage, time, and pressure.

The apparatus consists of two flat aluminum plates (for the sandwich), a regulated power supply source, a rheostat, a milliammeter, and a voltmeter (fig. 13).

To assemble the sandwich, an aluminum plate (cathode) is placed at the bottom on an insulating plate (fig. 14). A pad consisting of the printing medium and a soft backing paper immersed in $K_4Fe(CN)_6$ is drained, blotted, and placed on the aluminum plate with the printing surface up. The specimen (anode) and a second aluminum plate are placed on top. A 10-pound weight is placed on top to ensure better contact of the surfaces. The circuit (6 volts) is closed for 1 to 30 seconds and then broken again. A print is thus obtained on the printing medium. To ensure the best possible prints, the printing medium should be applied to the specimen first, and rubber rollers should be used to work out any trapped air bubbles. Iron from $FeSO_4 \cdot nH_2O$ (the pyrite oxidation product) is reproduced as blue ferric ferrocyanide when contacting $K_4Fe(CN)_6$, which

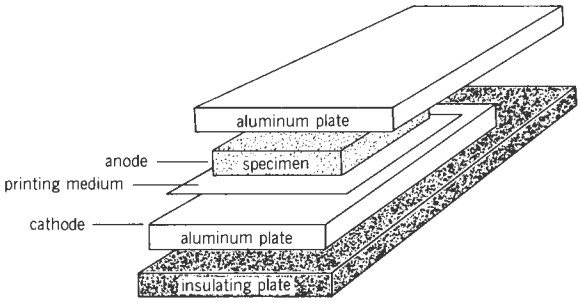

Figure 14. Expanded view of the sandwich used in electrographic analysis.

serves both as electrolyte and color-producing reagent. Both Kodak dye transfer paper and stripping film were used as a printing medium. The paper made sharper and more contrasting prints, but the film was used if a transparent background was required.

The 20 samples of pyrite were imbedded in bioplastic with two sides of the pyrite polished and exposed. Each imbedded block was placed in the electrograph sandwich (fig. 14). All factors (current, voltage, type of pyrite, etc.) being equal, the color intensity of a print for any sample depends on the length of time current passes through it. A portion of a pyrite sample undergoing very little oxidation appears very light blue or bluish yellow in a print, but a portion undergoing greater oxidation appears as a darker shade of blue.

The intensity of this blue color depends directly on the amount of iron reacting with $K_4Fe(CN)_6$, which is a measure of the oxidation. To measure the relative rate of oxidation of different types of pyrite in a sample, transparent prints were made by using stripping film. These transparent prints were subsequently run on a Jarrell-Ash densitometer, and the different color densities were recorded. This record gives a quantitative estimate of relative rates of oxidation of various forms of pyrite in a sample.

The clear part of the transparent slide on which the print was mounted for densitometer measurements was adjusted to 100-percent transmission for that print. A visual inspection of the prints showed that, basically, the prints consisted of three major divisions as far as color density was concerned: dark blue, medium blue, and light blue. Densitometer measurements revealed that more than 95 percent of the area of prints could be assigned to three divisions of color density: dark blue with 4- to 16-percent transmission, medium blue with 18- to 34-percent transmission, and light blue with 36- to 45-percent transmission of light. The three categories listed above were distinguished primarily on the basis of the light-transmission readings from the densitometer (table 5).

The terms "dark blue," "medium blue," and "light blue" were translated to mean highly oxidizable, moderately oxidizable, and weakly oxidizable (table 5). Thus from the results of electrographic analysis, pyrite samples were divided into these three groups based on the rate of oxidation. As one can see in table 5, most of the polished blocks have more than one kind of pyrite classified according to the rate of oxidation.

X-RAY ANALYSIS

To investigate further whether pyrite of different crystal size and purity and with different rates of oxidation might show different mineralogic characteristics, an X-ray analysis was made for each of the 20 samples which had been subjected to petrographic and electrographic analysis. It was assumed that if the differences in rates of oxidation were also influenced by the mineralogic aspect of pyrite, then pyrite with different rates of oxidation could be distinguished on the basis of unit cell size and crystallinity.

By using the data derived from the petrographic and electrographic studies and by using a small dentist's drill and special extracting tools, pyrite samples were extracted from exact locations of each rate of oxidation in the sample. A few samples had pyrite which had a uniform rate of oxidation, and thus they afforded only one pyrite sample for X-ray analysis. Others had two or three rates of oxidation distinguishable on electrographic prints. From the latter, one sample for X-ray analysis was taken from each oxidation-rate category. This method of separation yielded 48 samples for X-ray study. Each of these samples was labeled with the number of the main sample from which it was taken and with a suffix indicating if it was highly oxidizable (HO), moderately oxidizable (MO), or weakly oxidizable (WO).

A Norelco diffractometer was used for this study. The machine settings were as follows:

Radiation	Iron
Filter	Manganese
KVP	35 KV
Current	18 Ma
Scale factor	'8'
Multiplier	'.8'
Time constant	'8'
Diffraction speed	$1°2\theta$/min

Sodium chloride was added to each sample as an internal standard. This was done to overcome possible machine misalignment. The samples were run from

Table 5. Densitometer measurements of three categories of 20 pyrite samples

Category	Percentage of transmission of light																			
	Sample																			
	1	2	3	4	5	6	7	8	9	10	11	12	13	14	15	16	17	18	19	20
Highly oxidizable	6- 8	5- 9	5-14	4-15	10-16	6-14	10-16	8-10	——	——	——	——	——	——	——	11-15	7-15	4-16	7- 9	——
Moderately oxidizable	23-24	19-22	19-29	28-33	29-34	25-30	21-26	19-21	24-29	——	——	20-30	20-34	21-29	18-29	24-32	22-26	19-29	20-29	29-34
Weakly oxidizable	41-43	40-43	38-45	40-45	40-45	38-45	35-39	36-38	36-40	40-45	38-45	40-45	——	41-44	——	40-45	39-42	38-49	——	42-44

Table 6. Unit cell edge of pyrite as computed from (311) peak of sample 7

Unit cell from ASTM	Category	Unit edge measured	Difference from ASTM
5.417 Å	HO	5.439 Å	+ 0.0022
	MO	5.427 Å	+ 0.001
	WO	5.409 Å	- 0.0008

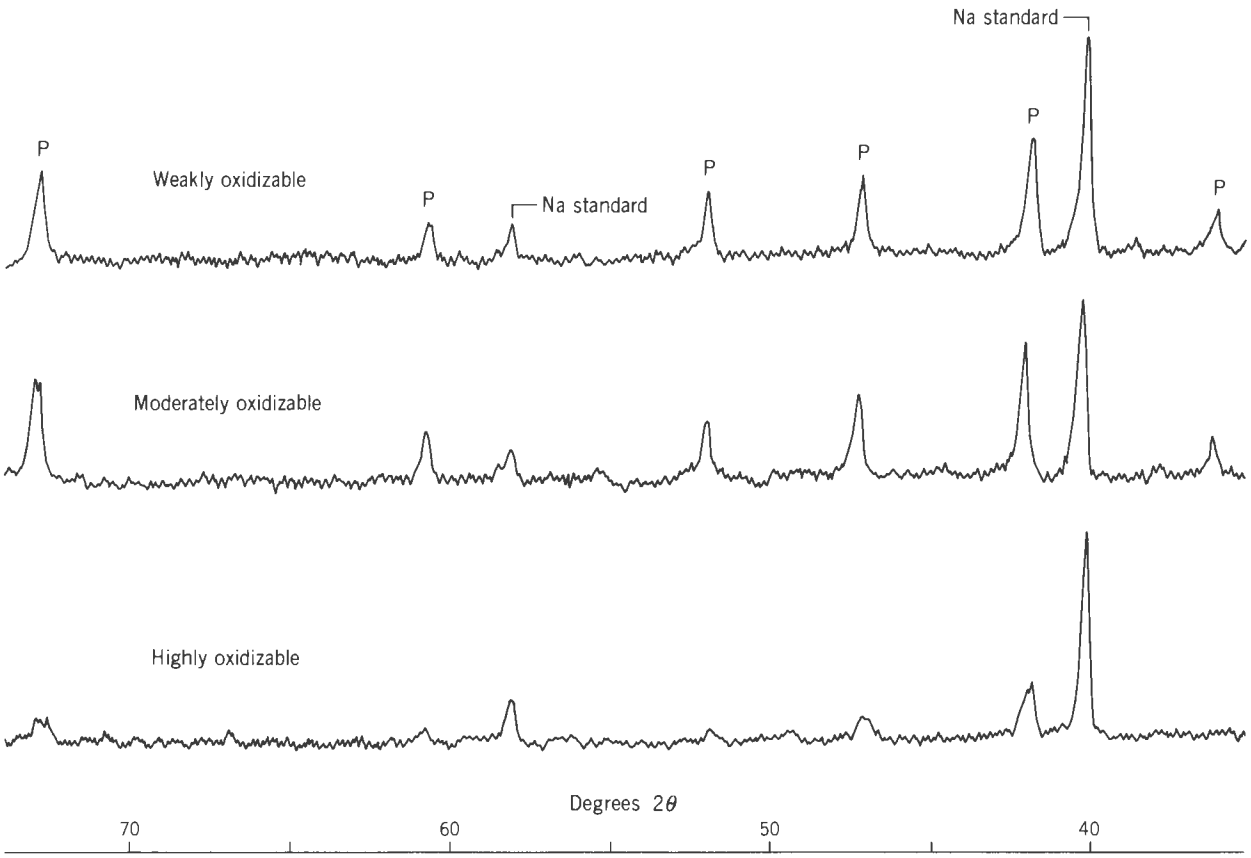

Figure 15. X-ray diffraction traces of weakly oxidizable, moderately oxidizable, and highly oxidizable categories of pyrite (2θ Fe Kα). P indicates pyrite peaks.

4° two theta to 75° two theta. The reason diffraction was started at 4° two theta was to check for any clay minerals present. FeS_2 (311) peak was selected for computing the unit cell dimensions. The shapes and intensities of FeS_2 (311) and (200) peaks were studied for relative crystallinity of pyrite samples with different relative oxidation rates. The shape of the peak was studied by computing a ratio of width at half maximum to the width at the base of each peak.

Preliminary inspection of diffraction charts indicated that the "d" spacings of HO, MO, and WO categories of pyrite were not significantly different. It seemed that to compute unit cell size for each sample for comparison would not be advisable, because the difference in "d" spacings measured was very small and it could not be said whether this represented a real difference in unit cell dimensions or was the result of inherent error in measurement due to rather poor peak of many samples. In view of this, only sample 7 was selected for unit cell measurement. This sample had all three (HO, MO, and WO) categories and gave fairly good peak for each one.

Table 7. Ratio of width at one-half maximum to width at base of peak for 20 pyrite samples

Sample No.	Weakly oxidizable (WO)	Moderately oxidizable (MO)	Highly oxidizable (HO)
1	.285	.357	.381
2	.341	.46	.582
3	.33	.42	.463
4	.301	.391	.521
5	.38	.387	.543
6	.361	.46	.58
7	.296	.442	.581
8	.312	.42	.56
9	.33	.45	——
10	.316	——	——
11	.35	——	——
12	.391	.481	——
13	——	.461	——
14	.411	.443	——
15	——	.5	——
16	.296	.491	.61
17	.4	.472	.67
18	.36	.48	.72
19	——	.41	.64
20	.4	.49	——

The results are shown in table 6. The unit cell edge appears to be larger for the highly oxidizable (HO) category, smaller for the moderately oxidizable (MO), and still smaller for the weakly oxidizable (WO). These results are very close to the unit cell edge of pyrite as reported on the reference card set published by the American Society for Testing and Materials.

The intensities and shapes of the peaks from pyrite with different rates of oxidation are strikingly different (fig. 15). The ratio of width at one-half maximum to width of base of peak (table 7) does not show a distinct numerical separation of the three categories. In general, HO has a much higher ratio than the MO and WO categories. This signifies that category HO has pyrite with a lesser degree of crystallinity than the other two categories have. The WO pyrite appears to have the highest degree of crystallinity. This is also confirmed by the observed intensities of the peaks. Category HO has the lowest intensity for the peaks among the three categories (fig. 15). The combination of low intensity and broad peaks suggests clearly that the HO pyrite has the lowest crystallinity of the three categories. A comparison of the other two categories indicates that MO pyrite has a lower crystallinity than WO pyrite.

COMPARISON OF PETROGRAPHIC, X-RAY, AND ELECTROGRAPHIC ANALYSES

The petrographic study shows that pyrite occurs in a wide range of crystal size and that its purity is far from uniform. The petrographic composition of any one sample ranges from relatively pure pyrite to a mixture of pyrite, inorganic material (mostly clay), and coaly material.

The electrographic study shows that pyrite can be classified on the basis of its rate of oxidation. A comparison of the crystal size and purity of pyrite as determined in the petrographic study and its rate of oxidation reveals that there is a correlation between them. In every sample the highly oxidizable pyrite is less than 10 microns in crystal size. It is associated with coaly material in most samples and with other inorganic materials (probably clay) in a few. Moderately oxidizable pyrite has a crystal size in the 15- to 25-micron range and very little coaly or inorganic material associated with it. The weakly oxidizable pyrite has a crystal size larger than 25 microns and no coaly or inorganic material associated with it. Pyrite as cleat fillings in general shows very little oxidation, but lenticular pyrite has a higher rate of oxidation. Recrystallized pyrite shows practically no oxidation relative to other forms of pyrite.

The X-ray study shows further evidence of the effect of crystallinity and unit cell dimensions of pyrite as an influence on its rate of oxidation. Although nothing definite can be concluded about the unit cell size of pyrite and its relation to the rate of oxidation, probably the larger the unit cell size, the higher the rate of oxidation.

A lower degree of crystallinity is associated with a high rate of oxidation. The least oxidizable pyrite appears to have the highest degree of crystallinity of the three categories; this is evident both by sharp peaks and relatively high intensity. Pyrite of category HO has a small crystal size (less than 10 microns) and low crystallinity; pyrite of category MO has a crystal size between 15 and 25 microns and higher crystallinity than category HO; pyrite of category WO has the largest crystal size of the three categories (greater than 25 microns) and the highest degree of crystallinity.

Literature Cited

Ashley, G. H.
1919 - Sulphur in coal, geological aspects: Am. Inst. Mining Metall. Engineers Trans., v. 63, p. 732-738.

Bain, C. W.
1935 - Pyrite oxidation: Econ. Geology, v. 30, p. 166-169.

Braley, S. A.
1960 - The oxidation of pyritic conglomerates: Rept. on Research Proj. 370-6, Mellon Inst.

Cady, C. H.
1935 - Distribution of sulphur in Illinois coals and its geological implications: Illinois Geol. Survey Rept. Inv. 35, p. 23-29.

Dove, L. P.
1919 - Pyrite in the coals of Indiana: Indiana Yearbook for 1918, p. 219-238.

Fritz, Helmut
1929 - Studien uber die Empfindlichkeit einiger characteristischer chemischer Farbreaktioner mit Hilfe der Elektro-tuffelmethode: Zeitschr. anal. Chemie, v. 78, p. 418-427.

Glazunov, A.
1929 - Electrochemical reproduction of macrostructure: Chimie et industrie, spec. no. 425.

Gottschalk, V. H., and Buehler, H. A.
1912 - Oxidation of sulphides: Econ. Geology, v. 7, p. 15-34.

Gray, R. J., and others
1963 - Distribution of forms of sulphur in high volatile Pittsburgh seam coal: Soc. Mining Engineers Trans., v. 226, 113 p.

Hermance, H. W., and Wadlow, H. V.
1951 - Electrography and electrospot testing, *in* Berl, W. G., ed., Physical method in chemical analysis: New York, Academic Press Inc., v. 2, p. 156-227.

Holbrook, E. A.
1919 - Experiments on the concentration of pyrite from Indiana: Indiana Yearbook for 1918, p. 239-255.

McKay, D. R., and Halpern, Jack
1958 - A kinetic study of the oxidation of pyrite in aqueous suspension: Am. Inst. Mining Metall. Petroleum Engineers Trans., v. 212, p. 301-309.

Neavel, R. C.
1961 - Petrographic and chemical composition of Indiana coals: Indiana Geol. Survey Bull. 22, 81 p.

Nelson, H. W., and others
1933 - Oxidation of pyrite sulphur in bituminous coal: Indus. and Eng. Chemistry, v. 25, p. 1355-1358.

Newhouse, W. H.
1927 - Some forms of iron sulfide occurring in coal and other sedimentary rocks: Jour. Geology, v. 35, p. 73-83.

Powell, A. R., and Parr, S. W.
1919 - A study of the forms in which sulphur occurs in coal: Illinois Univ. Eng. Expt. Sta. Bull. 111, 62 p.

Rossetti, Vasco, and Cesini, A. M.
1957 - Electrochemical effects between metal sulfides in mine water: Periodico Mineral (Rome), v. 26, 63 p.

Sato, Motoaki
1960 - Oxidation of sulfide ore bodies II: Oxidation mechanism of sulfide minerals at 25° C: Econ. Geology, v. 55, p. 1202-1231.

Shrock, R. R., and Malott, C. A.
1929 - Structural features of West Franklin formation of southwestern Indiana: Am. Assoc. Petroleum Geologists Bull., v. 13, p. 1301-1315, 3 figs.

Silverman, M. P., and Ehrlich, H. L.
1964 - Microbial formation and degradation of minerals: Appl. Microbiology, v. 6, p. 153-206.

Silverman, M. P., Rogoff, M. H., and Wender, Irving
1963 - Removal of pyritic sulfur from coal by bacterial action: Fuel, v. 42, p. 113-124.

Sprunk, G. C., and O'Donnell, H. J.
1942 - Mineral matter in coal: U.S. Bur. Mines Tech. Paper 648, 66 p.

Stenhouse, J. F., and Armstrong, W. M.
1952 - The aqueous oxidation of pyrite: Canadian Mining Metall. Bull. 45, p. 49-53.

Stokes, H. N.
1907 - Experiments on the action of various solutions on pyrite and marcasite: Econ. Geology, v. 2, p. 14-23.

Thiessen, Reinhardt
1919 - Occurrence and origin of finely disseminated sulphur compounds in coal: Am. Inst. Mining Metall. Engineers Trans., v. 63, p. 913-931.

Tucker, W. M.
1919 - Pyrite deposits in Ohio coal: Econ. Geology, v. 14, p. 198-219.

Waddell, Courtney
1954 - Geology and coal deposits of the Shelburn Quadrangle, Sullivan County, Indiana: U.S. Geol. Survey Coal Inv. Map C-17.

Winchell, A. N.
1907 - The oxidation of pyrite: Econ. Geology, v. 2, p. 290-294.

Yancey, H. F., and Fraser, Thomas
1921 - The distribution of the forms of sulphur in the coal beds: Illinois Univ. Eng. Expt. Sta. Bull. 125, 94 p.

Yancey, H. F., and Parr, S. W.
1927 - Sulphur forms in coal: their distribution and control: Indus. and Eng. Chemistry, v. 16, 501 p.

THIS PAGE INTENTIONALLY LEFT BLANK

APPENDIX: A BRIEF PETROGRAPHIC DESCRIPTION OF THE 20 SAMPLES STUDIED

Sample 1. Pyrite was present as a thick band, about 2 cm thick, bounded on both sides by minor cleats. Pyrite in the band had crystal size ranging from 1 to about 50 microns. Some extraneous matter mixed with pyrite was visible. Pyrite in the cleats had crystals ranging from 10 to 40 microns and showing a definite elongation perpendicular to the bedding.

Sample 2. This sample consisted of a thick lens of pyrite. Crystal size ranged from 1 to less than 60 microns. There was evidence of some recrystallization of pyrite which generally had a crystal size larger than 35 microns. No cleats were visible. Coal and inorganic matter was admixed with pyrite.

Sample 3. Pyrite was in the form of a network of cleats and thin lenticular bands. The bands ranged from one-half mm to about 5 mm in thickness. The crystal size in the lenticular bands ranged from 1 micron to more than 30 microns. The average crystal size in the cleats was about 40 microns. Pyrite in the bands was highly impure, and inorganic matter and coal were the main impurities.

Sample 4. Pyrite in sample 4 occurred as a major lenticular lens and network of cleats. The pyrite in the lenticular lens had replaced fusinite, and cell structure was evident. The crystal size in the lens ranged from 5 to 60 microns. Pyrite was generally of high purity, showing well-developed crystals. The crystal size of the pyrite in the cleats ranged from 15 to 35 microns.

Sample 5. Pyrite in this sample consisted of a thick lenticular band about 3 cm thick. The crystal size ranged from less than 1 to 40 microns. The pyrite had very little coal or inorganic matter associated with it except in the uppermost part of the band where the crystal size was smallest.

Sample 6. Pyrite was in a band about 10 cm thick. The crystal size ranged from less than 1 to 40 microns. Recrystallized pyrite was present; the size of each crystalline mass averaged more than 50 microns. No cleats were evident.

Sample 7. Pyrite in this sample consisted of numerous thin interconnected lenticular bands. The crystal size ranged from less than 1 to 50 microns. There was some recrystallized pyrite in the bands. Minor cleats were also present. The crystal size in the cleats averaged about 40 microns.

Sample 8. This sample consisted of five lenticular bands of pyrite connected by a network of cleats. Each band was about 1.5 to 2 mm thick. The pyrite in the bands was highly impure, mixed mostly with inorganic matter. Crystal size in the bands ranged from less than 1 micron to about 30 microns. The pyrite in the cleats had an average size of 40 microns.

Sample 9. Pyrite was present in the form of numerous very thin lenticular bands with an average thickness less than .5 mm. The pyrite in the bands was very impure and was mixed with coal and inorganic matter. The crystal size ranged from less than 1 micron to 20 microns. No cleats were visible.

Sample 10. Pyrite was in the form of a 2-cm-thick lenticular band. The crystal size ranged from 50 microns to less than 1 micron. Pyrite was mixed with inorganic matter and coal. There were no cleats.

Sample 11. The sample consisted of a 2-cm-thick lenticular band of pyrite. Pyrite had replaced plant material, and cell structure was evident throughout the lens. The crystal size ranged from less than 1 micron to 50 microns. No cleats were visible. The pyrite had inorganic matter mixed with it.

Sample 12. The sample consisted of thin lenticular bands interconnected by numerous cleats. Pyrite in the bands was of good purity and ranged from less than 1 micron to 60 microns in crystal size. Cleats had an average size of about 30 microns. Very little inorganic matter or coal was mixed with the bands.

Sample 13. Pyrite in this sample was in the form of small disconnected lenses. The pyrite was mostly less than 15 microns in crystal size. These lenses had a fair amount of inorganic matter mixed with them. No cleats were visible.

Sample 14. Pyrite was in the form of a single 2-mm-thick band. Pyrite was of high purity; very little coal or inorganic matter could be seen associated with it. The crystal size ranged from less than 1 micron to 60 microns. There were no cleats.

Sample 15. Pyrite consisted of a network of cleats. The crystal size ranged from 75 to about 5 microns.

Sample 16. Pyrite was in the form of a thick band about 8 cm thick. Pyrite had mostly replaced plant material, and cell structure was present throughout the band. Inorganic matter was present in subordinate amounts. The crystal size ranged from less than 1 micron to 60 microns. Very little coal could be seen, and no cleats were observed.

Sample 17. Pyrite was in the form of a thick lens about 2 cm thick. The crystal size ranged from about less than 1 micron to 45 microns. Very little cell structure could be seen. Some recrystallized pyrite was present. No cleats were observed.

Sample 18. Pyrite was in the form of a 2-mm-thick band. Most of the pyrite in the band was recrystallized. The recrystallized pyrite had an average crystal size of about 50 microns, and the rest of the pyrite ranged from about less than 1 micron to 45 microns in crystal size. Very little inorganic matter was observed; however, coal, mixed with pyrite, was present in minor quantities. No cleats were visible.

Sample 19. Pyrite was in the form of five thin (1 mm) bands. The crystal size ranged from less than 1 micron to 40 microns. The pyrite was mixed with inorganic matter and coal. No cleats were present.

Sample 20. Pyrite consisted of a thick 5-cm band. The crystal size ranged from less than 1 micron to 45 microns. Very little coal was associated with pyrite; however, there was some inorganic matter with it. No cleats were present.

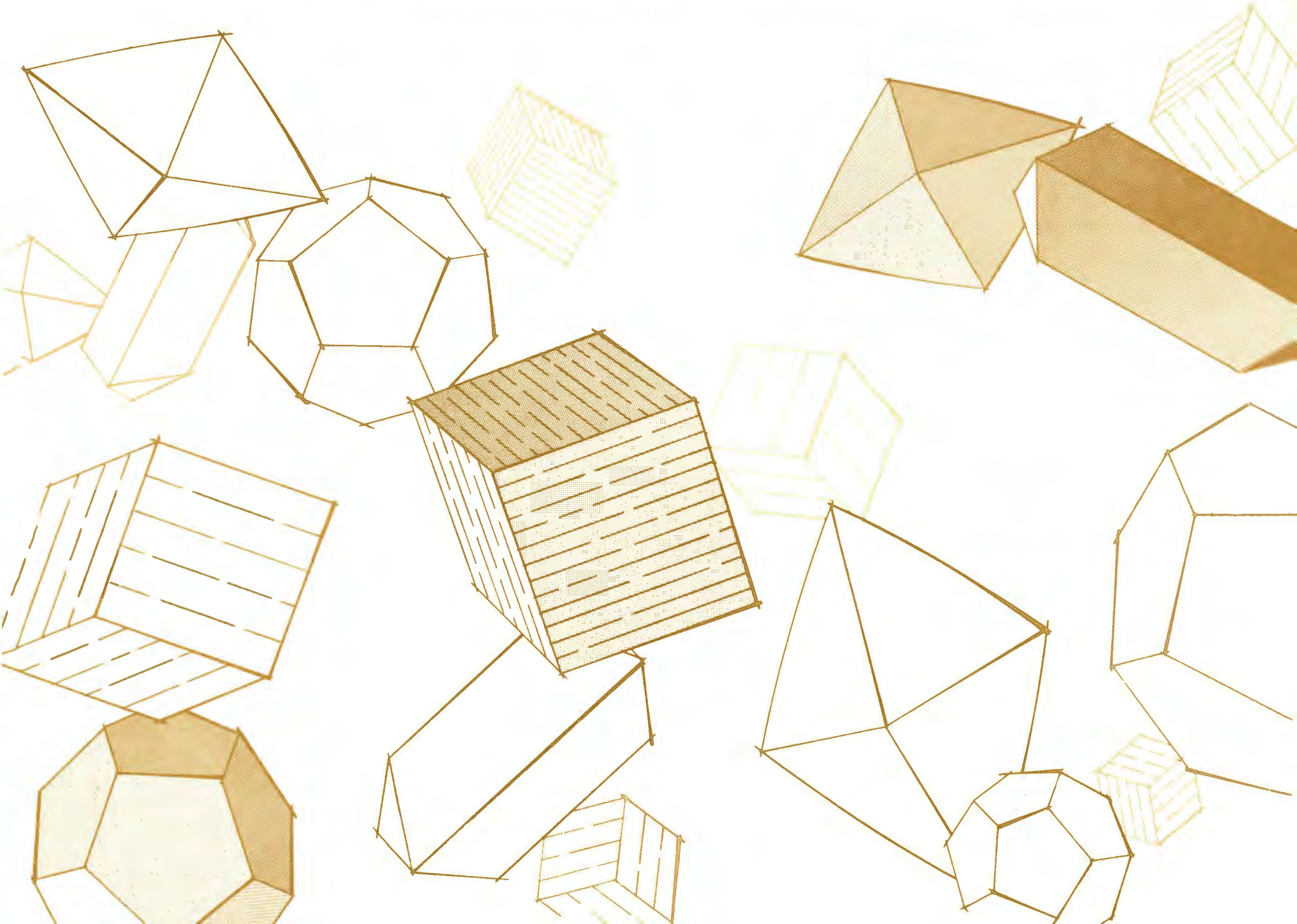

OVERSIZED DOCUMENT

The following pages are oversized and need to be printed in correct format.

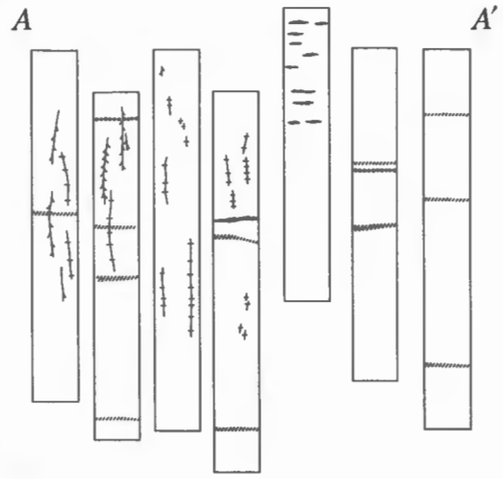

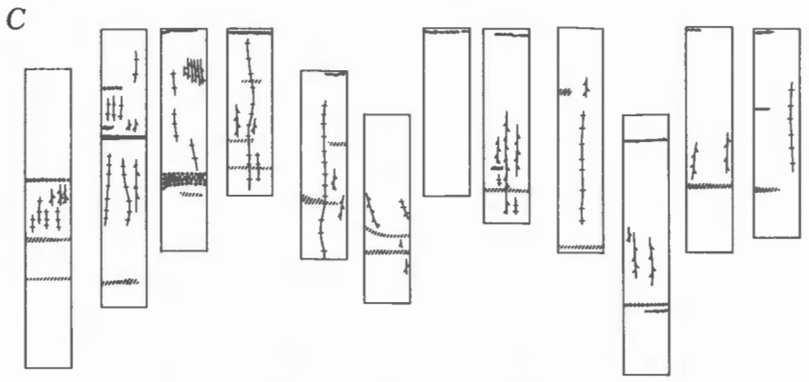

Differences in vertical position of columns represent from 3 to 15 feet of local relief. That is, columns that are plotted the highest are on hills in the mine and columns plotted the lowest are in valleys.

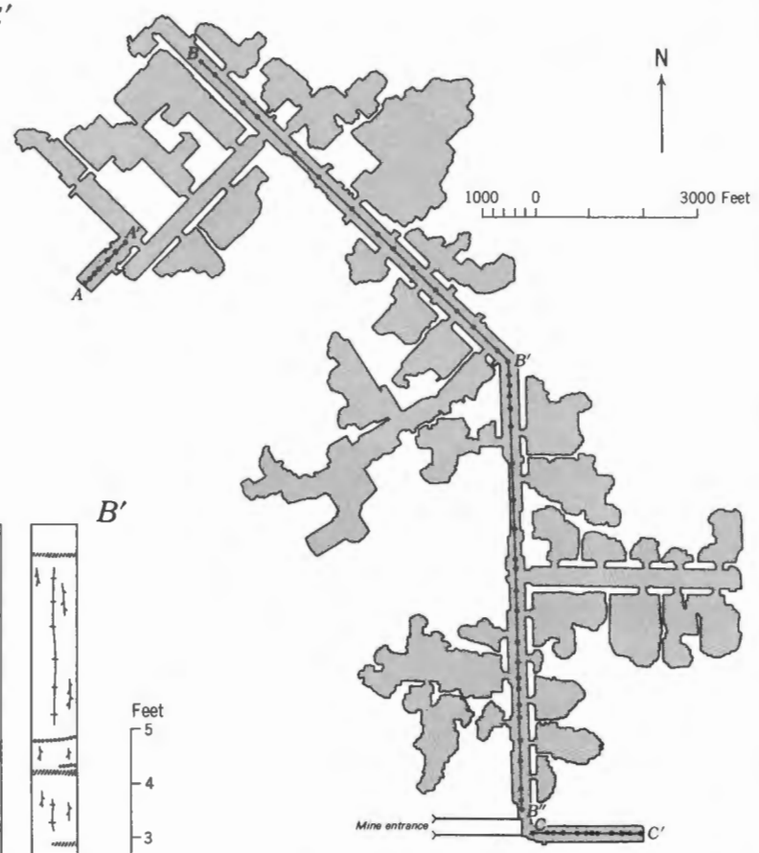

MAP OF THUNDERBIRD MINE AREA SHOWING LOCATION OF SECTIONS A-A′, B-B′-B″, AND C-C′

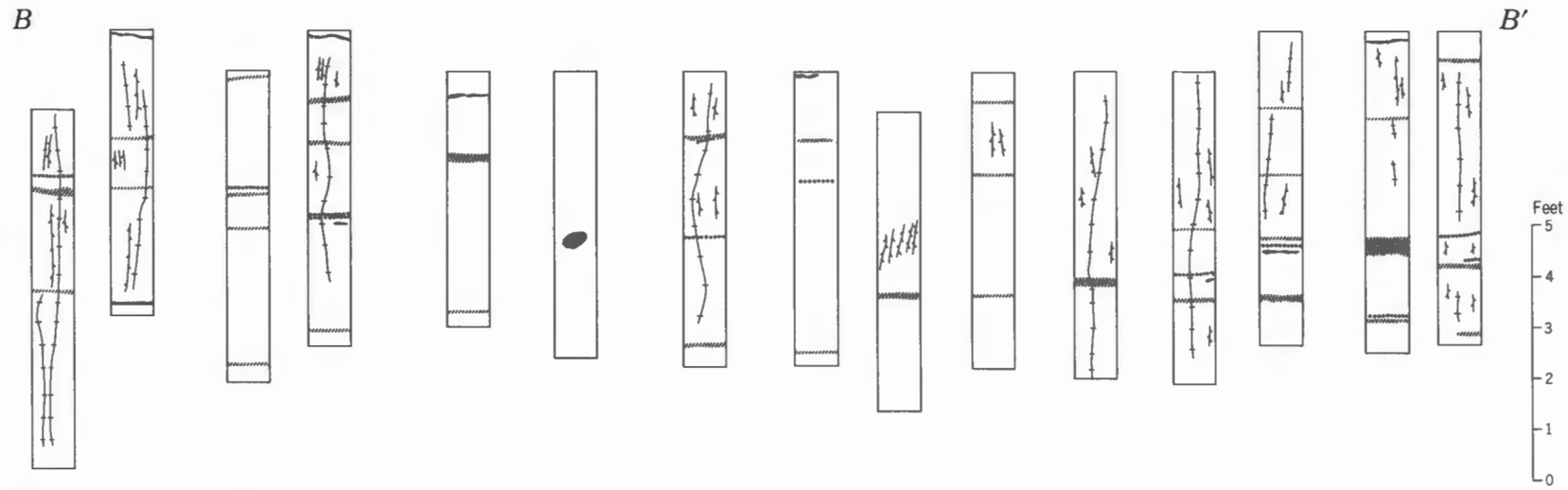

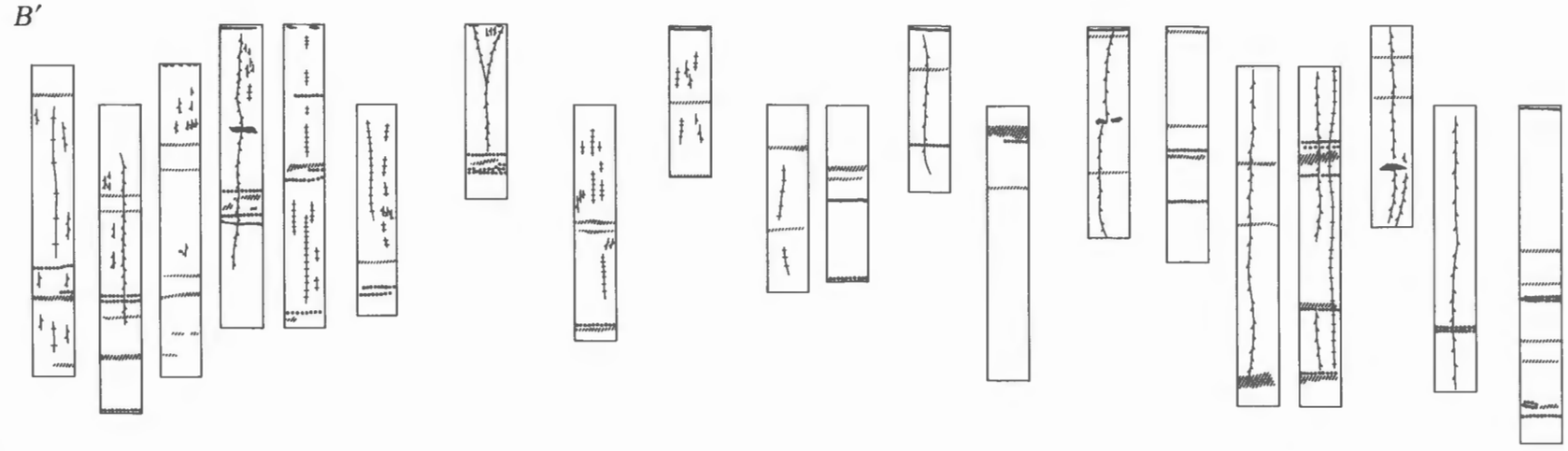

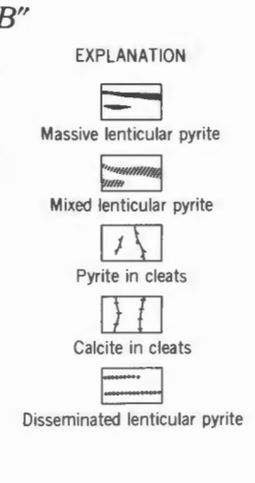

GRAPHIC REPRESENTATION OF DATA FROM PYRITE DISTRIBUTION STUDY OF SPRINGFIELD COAL MEMBER (V), THUNDERBIRD MINE, SULLIVAN COUNTY, INDIANA